HOFMANN, K. A. & HOCCHTLEN, F. (1903). *Ber. Dtsch. Chem. Ges.* **36**, 1149.
HOWARD, C. J., BALL, C. J., DAVIS, R. L. & ELCOMBE, M. M. (1983). *Aust. J. Phys.* **36**, 507–518.
RAYNER, J. H. & POWELL, H. M. (1952). *J. Chem. Soc.* pp. 319–328.
SASAKI, Y. (1969). *Bull. Chem. Soc. Jpn*, **42**, 2412.
WEGENER, W., BOSTOEN, C. & CODDENS, G. (1990). *J. Phys. Condens. Matter*, **2**, 3177–3185.

Acta Cryst. (1994). B**50**, 435–441

Synchrotron X-ray Study of the Electron Density in α-Fe_2O_3

BY E. N. MASLEN, V. A. STRELTSOV* AND N. R. STRELTSOVA

Crystallography Centre, University of Western Australia, Nedlands 6009, *Australia*

AND N. ISHIZAWA

Research Laboratory of Engineering Materials, Tokyo Institute of Technology, 4259 *Nagatsuta, Midori-Ku, Yokohama* 227, *Japan*

(*Received* 16 *November* 1993; *accepted* 23 *February* 1994)

Abstract

Structure factors for synthetic haematite, α-Fe_2O_3, have been measured for two small crystals using focused $\lambda = 0.7$ Å synchrotron radiation. The structure factors from the two data sets are consistent. Approximate symmetry in the concordant densities, related more closely to the Fe—Fe geometry than to the nearest-neighbour Fe—O interactions, is similar to that in the corundum α-Al_2O_3 structure. Deformation density maxima are located at the midpoint of the Fe—Fe vector along the c axis, on a common face for O-octahedra, perpendicular to c. Maxima also occur at the midpoint of the Fe–Fe vector bisecting the edges of the O-octahedra. These results are in accordance with theoretical predictions for metal–metal bonding. Space group $R\bar{3}c$, hexagonal, $M_r = 159.7$, $a = 5.0355$ (5), $c = 13.7471$ (7) Å, $V = 301.88$ (7) Å^3, $Z = 6$, $D_x = 5.270$ Mg m^{-3}, $\mu_{0.7} = 13.68$ mm^{-1}, $F(000) = 456$, $T = 293$ K, $R = 0.019$, $wR = 0.021$, $S = 5.55$ for 368 unique reflections in the most accurate data set 2.

Introduction

The deformation density ($\Delta\rho$) near the Al cations for α-Al_2O_3, observed by Maslen, Streltsov, Streltsova, Ishizawa & Satow (1993), has approximate sixfold symmetry. That unexpected topography may be significant to our basic understanding of bonding in solids. It should, therefore, be tested by imaging the electron densities in related compounds. The c/a ratios for most corundum oxide structures, including α-Al_2O_3, α-Fe_2O_3, Cr_2O_3, Ga_2O_3 and Rh_2O_3, range from 2.70 to 2.74 (Prewitt, Shannon, Rogers & Sleight, 1969). That ratio is anomalously small, 2.6388 (3), for Ti_2O_3 (Vincent, Yvon, Grüttner & Ashkenazi, 1980) and anomalously large, 2.8280 (3), for V_2O_3 (Vincent, Yvon & Ashkenazi, 1980). The corundum-type α-Fe_2O_3 unit cell is bigger than that for α-Al_2O_3, but the axial ratio c/a, determined to be 2.731 (1) for crystal (1) and 2.7300 (4) for crystal (2), is within 1 e.s.d. of $c/a = 2.7308$ (3) for α-Al_2O_3.

According to a schematic band structure proposed by Goodenough (1971) for corundum-type 3*d* crystals, the trigonally distorted octahedral crystal field quantized along the threefold axis splits the fivefold-degenerate 3*d* state into a stable σ-bonding pair of e_g orbitals directed toward the nearest-neighbour O atoms, a pair of e_t orbitals directed approximately towards three neighbouring cations in a puckered basal plane through common octahedral site edges, and an a_t orbital directed along the c axis towards one near-neighbour through a common octahedral site face. From symmetry considerations alone, the energy band scheme shows that the bonding a_t and e_t band overlap depends on the c/a ratio and on the widths of these bands.

In theory, the a_t and e_t orbitals for α-Fe_2O_3 are both half filled. Any variation in the c/a ratio that stabilized one would be at the expense of the other. The small c/a ratio of Ti_2O_3 stabilizes a filled and bonding a_t band at the expense of empty e_t bands. The large c/a ratio of V_2O_3 stabilizes the two bonding e_t orbitals per cation relative to the lower a_t band. Experimentally determined $\Delta\rho$ maps for Ti_2O_3 (Vincent, Yvon, Grüttner & Ashkenazi, 1980) and for V_2O_3 (Vincent, Yvon & Ashkenazi, 1980) support

* Author to whom correspondence should be addressed.

the existence of metal–metal bonds across the faces (Ti_2O_3) and edges (V_2O_3) of the O-octahedra. That explains why the c/a ratio is anomalously low for Ti_2O_3 and high for V_2O_3.

From similar considerations one could expect α-Fe_2O_3 to show metal–metal interactions of both types, characterized by increased positive density at the midpoint of the cation–cation contacts. The deformation density for α-Fe_2O_3 at room temperature was measured by X-ray diffraction experiments with an X-ray tube source by Antipin, Tsirelson, Flyugge, Gerr, Struchkov & Ozerov (1985) and by Tsirelson, Antipin, Streltsov, Ozerov & Struchkov (1988) at 153 K (below the flip-spin transition) using the same spherical sample ($r = 0.15$ mm). Zachariasen (1967) type extinction corrections were determined as part of the structure refinements. Those $\Delta\rho$ maps are consistent, conforming to the space-group symmetry and showing evidence for Fe—Fe bonding only along the c axis.

Although α-Fe_2O_3 is isostructural with α-Al_2O_3, it differs markedly from the latter compound by more readily forming near-perfect crystals. X-ray diffraction data from these crystals are strongly affected by extinction, which provides a means to assess the degree of dependence of the measured $\Delta\rho$ topography on the crystal's mosaic structure.

Experimental

Intensities of reflections that are equivalent by symmetry were measured for several crystals grown by a range of techniques. Equivalent Bragg reflections, including Friedel-related equivalents, with moderate intensity agreed closely for most crystals, but that agreement deteriorated rapidly with increasing intensity. Because current diffraction theories do not permit extinction corrections to be determined reliably in such cases, these crystals were not suitable for accurate imaging of the deformation density.

The agreement between Friedel-related intensities for crystals extracted from a sample prepared by gaseous diffusion in the Institute of Information at the MIREA, Moscow, was satisfactory. Two small specimens with natural faces selected for quantitative X-ray diffraction measurements were bounded by two $\{0\bar{1}2\}$, two $\{\bar{1}02\}$, two $\{1\bar{1}2\}$ and one $\{2\bar{1}0\}$ faces for crystal (1) and two $\{003\}$, two $\{0\bar{1}2\}$, two $\{\bar{1}02\}$, two $\{1\bar{1}2\}$ and one $\{1\bar{1}2\}$ faces for crystal (2). The dimensions $14 \times 14 \times 14 \times 10$ μm and $30 \times 22 \times 20 \times 20 \times 25$ μm from the crystal centre were measured and the faces indexed using optical and scanning electron Philips SEM505 microscopes, for crystals (1) and (2), respectively.

Diffraction intensity data sets 1 and 2 were measured with synchrotron X-ray radiation of wavelength 0.7000 (2) Å using the BL14A four-circle diffractometer (Satow & Iitaka, 1989) at the Tsukuba Photon Factory. The vertically polarized synchrotron radiation beam from a vertical wiggler was monochromated by a double Si(111) crystal monochromator, using a curve mirror to focus the X-rays. The polarization ratio of 0.95 for the radiation is the fraction of the total incident beam intensity with its electric vector vertical. Since the stored positron beam decays exponentially with time, a monitor ion chamber was used to monitor the incident beam intensity. An incident beam slit, 0.4 mm in diameter, was installed before the monitor ion counter. The narrow pin-hole slit of 0.4 mm provides an adequately homogeneous and intense beam. The alignment of the first monochromator crystal as well as the vertical translations of the mirror were automatically optimized every 20 min during data collection by flux maximization. By positioning the specimen slightly off-focus, changes in the synchrotron radiation intensity due to instabilities in the particle beam were minimized. Through the automatic optics optimization, intensity stability of the incident beam is within 1% over a 1 day period. A 3×3 mm receiving slit was placed in front of the scintillation counter. Further experimental details are set out in Table 1.

Lattice constants were determined from six equivalent reflections at 2θ values of 84.7° for data set 1 and 114.7° for data set 2. Reflection intensities were measured systematically using $\omega/2\theta$ scans for the complete sphere of reciprocal space with $(\sin\theta/\lambda)_{max} = 1.094$ Å^{-1}, $-11 \le h \le 11$, $-11 \le k \le 11$, $-30 \le l \le 30$ for the two data sets. Six standard reflection intensities were measured every 100 reflections to monitor the stability of the incident beam. The measured intensities were modified for fluctuation of the standards and the variances adjusted as suggested by Rees (1977). Variances in the measured structure factors evaluated from counting statistics were modified for source instability, as indicated by the standards. Reflections having measured variances consistent with Poisson statistics were assigned that variance. Variances for the other reflections were increased when necessary, according to the scatter of equivalents following a Fisher test.

Lorentz and polarization were applied. Absorption corrections (Alcock, 1974) were evaluated analytically. The reference state for structure-factor calculations was the independent atom model (IAM) evaluated using spherical atomic scattering factors from *International Tables for X-ray Crystallography* (Vol. IV, 1974), with dispersion corrections $\Delta f'$, $\Delta f''$ of 0.343, 0.826 for Fe and 0.011, 0.006 for O at 0.7 Å, evaluated by Creagh (1992). All subsequent calculations utilized the *Xtal*3.2 System of Crystallographic Programs (Hall, Flack & Stewart, 1992)

Table 1. *Experimental and refinement data for* α-Fe_2O_3

	Crystal (1)	Crystal (2)
Radiation	Synchrotron	Synchrotron
λ (Å)	0.7000 (2)	0.7000 (2)
Diffractometer	PF†	PF†
Monochromator	Si(111)	Si(111)
Scan speed (° min^{-1})	16	16
Peak scan width ($a + b \tan\theta$)	0.3; 0.0	0.35; 0.0
Maximum 2θ(°)	100	100
Max. intensity variations of standards [±(606), ±(6̄66), ±(06̄6)] (%)	3.4	3.6
Instability factor c from standards [$\sigma^2(I) = \sigma^2_{counts} + cI^2$]	6.54×10^{-4}	4.2×10^{-4}
Reflections measured	3910	3924
Transmission range min./max.	0.693/0.750	0.590/0.643
Independent reflections	362	368
$R_{int}(F^2)$ (before, after absorption)	0.046, 0.045	0.036, 0.035
Conventional refinement with scale factor fixed		
Number of parameters	9	9
Extinction,‡ r^*	1.06 (6) × 10^4	3.2 (1) × 10^4
Min. Extinction$y$,§ (hkl)	0.73, (01̄4)	[illegible] 3, (01̄4)
R	0.021	0.019
wR	0.020	0.021
S	3.28	5.55
Max. shift/e.s.d.	0.0014	0.0011
$\Delta\rho$, min./max. (e Å^{-3})	2.30/+0.70	−2.36/+1.13
$\sigma(\Delta\rho)$¶ (e Å^{-3})	0.14	0.10
Multipole refinement of $\Delta\rho$		
Number of parameters		38
R		0.018
wR		0.018
S		5.01

† The BL14A four-circle diffractometer (Satow & Iitaka, 1989) at the Tsukuba Photon Factory, Japan.

‡ Zachariasen (1967) extinction corrections included in least-squares structure refinement (Larson, 1970).

§ $F_{obs} = yF_{kin}$, where F_{kin} is the value of the kinematic structure factor.

¶ Mean e.s.d. value (Cruickshank, 1949).

implemented on Sun Sparc and DEC 5000/120 workstations.

Before structural parameters were refined, extinction correction of the full data sets from $|F_o|$ values based on equivalent reflection intensities (Maslen & Spadaccini, 1993) was attempted. The procedure, although developed for secondary extinction in small crystals, did not yield satisfactory results in this case. Haematite tends to form near-perfect crystals with irregularly located relatively large perfect domains, accounting for the significant differences between Friedel-related strong reflections observed for most specimens. Minor discrepancies persisted even in the samples selected for this study. Extinction corrections evaluated from intensities for equivalents may be hypersensitive to discrepancies of that type.

More robust, though biased, extinction correction can be evaluated by determination of the extinction parameters as part of a conventional least-squares refinement of the structural model. The widely invoked approaches by Zachariasen (1967) and Becker & Coppens (1974*a*,*b*) were applied using different models for the mosaic distributions of the micro-domains. The lowest y_{min} value of 0.42 determined by this method, for the crystal (2) 01̄4 reflection with the Becker & Coppens', type 1, Gaussian distribution, indicates severe extinction.

The $\Delta\rho$ maps were sensitive to the extinction model thus refined. Maps using the same extinction model for the two crystal data sets were dissimilar. Those from the present refinement with the Becker & Coppens', type 1, Gaussian distribution, extinction model for crystal (2) with the unreasonably low y_{min} value of 0.42, are broadly comparable with those for α-Fe_2O_3 presented by Antipin, Tsirelson, Flyugge, Gerr, Struchkov & Ozerov (1985) and Tsirelson, Antipin, Streltsov, Ozerov & Struchkov (1988), based on the Zachariasen (1967) type extinction correction refinement. This reduces our confidence in the significance of the $\Delta\rho$ maps reported previously.

The least-squares residuals for the α-Fe_2O_3 structure refinement were dominated extremely strongly by several low-angle reflections with high least-squares weights. In this situation, the parameters for the extinction models correlate strongly with the scale factor in the least-squares process, which reduces the dominance of the residuals as far as possible by optimizing the extinction parameter and the scale factor simultaneously. Least-squares methods may be biased significantly if large differences between the observed data and the model predictions occur more frequently than is predicted for a normal distribution. Where the sum of residuals is dominated by very few reflections, the least-squares process is so ill-conditioned that small adjustments to the model can alter the extinction correction and scale factor drastically. This introduces artefacts into difference-density maps (Streltsov & Maslen, 1992), as confirmed by the marked changes in $\Delta\rho$ topography resulting from modest changes in the weights of the large residual reflections.

The excessive correlation was reduced by refining each data set in two stages. First, the scale factor was determined by least-squares fitting, including the structural parameters but with fixed extinction parameters, for reflections with $\sin\theta/\lambda > 0.35$ (data set 1) and 0.6 Å^{-1} (data set 2), which are less strongly affected by extinction ($y_{min} > 0.8$) than are the intense low-angle reflections. The $y_{min} > 0.8$ criterion was established by preliminary refinements with the extinction parameter fixed at several values, spanning the range that could be obtained by refining the extinction correction with the structural parameters for all reflections. The extinction corrections were obviously over-estimated for some extinction parameter values within that range.

With the scale factor fixed at the first stage value, extinction parameters were then refined along with all the structural parameters. For each data set, nine independent parameters, including all the anisotropic

vibration tensor elements, were determined by full-matrix least squares refinement based on $|F|$, with weights equal to $1/\sigma^2(F_o)$ for all measured structure factors. The refined values are included in Tables 1 and 2.*

The $\Delta\rho$ maps for the two α-Fe_2O_3 crystals with the different extinction models refined in this way were remarkably consistent, in stark contrast to those with scale and extinction determined concurrently. This consistency justifies our reliance on the extinction corrections and scale factors evaluated using separate least-squares refinement of these parameters.

A local multipole expansion of the $\Delta\rho$ density obtained after IAM refinement in α-Fe_2O_3 for the data set of crystal (2), which was considered to be more accurate, was refined using the *VALRAY* programs (Stewart & Spackman, 1983). The scattering factors for neutral spherical Fe and O atoms were calculated from the Hartree–Fock atomic wavefunctions of Clementi (1965). The Fe atom in α-Fe_2O_3 is located on the threefold axis at 0,0,z, with the O atom at x,0,1/4 in the hexagonal setting of $R\bar{3}c$. To reduce extensive correlation in the least-squares refinement, the monopole populations for Fe and O were constrained by charge values, obtained from Hirshfeld partitioning of $\Delta\rho$ presented below. Dipoles (d_3) for Fe and (d_1) for O, quadrupoles (q_5) for Fe and (q_1, q_4, q_5) for O, octapoles (o_1, o_2, o_7) for Fe and (o_1, o_4, o_5) for O and hexadecapoles (h_3, h_4, h_9) for Fe and (h_1, h_4, h_5, h_8, h_9) for O were refined with reference to a Cartesian coordinate system with x parallel to a and z parallel to c. When populations and exponents for all these multipoles on both pseudo-atom types allowed by symmetry were included, along with positional and vibrational parameters, the model required a total of 38 variables. Convergence to a local minimum of the least-squares procedure based on $|F|$ with weights equal to $1/\sigma^2(F_o)$ for all measured structure factors was checked by including second derivatives in the final cycle of least squares (Spackman & Stewart, 1984).

Refinement of this multipole expansion was difficult. Due to the rather compact haematite structure, some pseudo-atom multipole functions overlap strongly. The locality principle that underlies the multipole expansion approach breaks down and consequently some refined parameters are strongly correlated. The refined parameters were sensitive to their initial values. The least-squares refinement process was so ill-conditioned that convergence was poor. The least stable variables in several refinements were the O-atom multipole parameters, whereas the Fe parameters were stable to within one standard deviation for all refinements, justifying the evalulation of 3*d*-orbital occupancies from multipole populations presented below.

Table 2. *Fractional coordinates and anisotropic vibration parameters from conventional* (I) *and multipole* (II) *refinement for* α-Fe_2O_3

	Crystal (1)	Crystal (2)	
	I	I	II
z(Fe)	0.35522 (1)	0.35528 (1)	0.35528 (1)
x(O)	0.69395 (10)	0.69397 (10)	0.69389 (9)
U_{11}(Fe)	0.00368 (3)	0.00334 (3)	0.00330 (3)
U_{33}(Fe)	0.00366 (3)	0.00344 (5)	0.00335 (4)
U_{11}(O)	0.00411 (10)	0.00376 (10)	0.00379 (9)
U_{22}(O)	0.00465 (15)	0.00417 (13)	0.00402 (12)
U_{33}(O)	0.00434 (11)	0.00416 (13)	0.00426 (13)
U_{13}(O)	0.00052 (6)	0.00059 (5)	0.00056 (5)

Refinement details are included in Tables 1 and 2. The maximum deviations between structural parameters from all refinements (Table 2) are 6 e.s.d.'s for z (Fe), 1 e.s.d. for x (O) and 10 e.s.d.'s for the temperature factors. Vibrational parameters from data set 2 are systematically lower than those from data set 1.

Structural parameters

The structural geometry for corundum is fully described in earlier literature, as indicated in the recent paper by Maslen, Streltsov, Streltsova, Ishizawa & Satow (1993). The O-atom geometry can be regarded as approximating hexagonal close packing, with the Fe atoms occupying two thirds of the trigonally-distorted octahedral interstices. Each Fe atom is surrounded by six O atoms. There are three at the corners of an equilateral triangle above the central Fe atom, with a shortest O—O contract of 2.6691 (6) Å. Each of those O atoms participates in an Fe—O bond of length 2.1141 (4) Å [1.9700 (2) Å in α-Al_2O_3]. The remaining three form another equilateral triangle below the central Fe atom, staggered with respect to the one above, with an O—O vector length of 2.8838 (4) Å. Each O atom in the second triangle is bound to Fe by a stronger Fe—O bond of length 1.9440 (3) Å [1.8525 (5) Å in α-Al_2O_3]. Each O atom is surrounded by four Fe atoms, two at 1.9440 (3) and two at 2.1141 (4) Å from the anion.

Each Fe atom in the α-Fe_2O_3 structure has ten Fe neighbours. The Fe—Fe vector along the threefold axis across the face shared by two FeO_6 coordination octahedra of 2.8945 (3) Å has the shortest Fe—Fe distance in the structure. The other three near-neighbour Fe—Fe vectors, 2.9692 (3) Å in length,

* Lists of structure factors for the two data sets and figures of deformation density sections in the (01$\bar{1}$0) plane through O and two Fe atoms for the extinction parameter included in the structure refinement have been deposited with the IUCr (Reference: AS0661). Copies may be obtained through The Managing Editor, International Union of Crystallography, 5 Abbey Square, Chester CH1 2HU, England.

are directed across the edges shared by FeO_6 octahedra in the basal plane. This shortest Fe—Fe distance in α-Fe_2O_3 is close to the Fe—Fe distance of 2.86645 (1) Å in crystalline α-Fe metal. The next six shortest Fe—Fe vectors, three of length 3.3617 (3) Å and three of length 3.7016 (3) Å, are directed across corners of the FeO_6 octahedra. The Fe—Fe distance along the threefold axis through the empty octahedral interstice is 3.9790 (3) Å.

Atomic charges and 3*d*-orbital population

Atomic charges listed in Table 3 were determined by projecting $\Delta\rho$ onto atomic density basis functions (Hirshfeld, 1977). The consistent results for both data sets suggest that electrons are transferred from the Fe cation to the O anion, by an amount almost twice that in α-Al_2O_3 (Maslen, Streltsov, Streltsova, Ishizawa & Satow, 1993).

The total population of the 3*d*-orbitals was normalized to six electrons, as for a spherical Fe atom. The 3*d*-orbital populations in α-Fe_2O_3 are presented in Table 3. The multipole populations for the Fe atom can be interpreted in terms of 3*d*-orbital occupancies using generalized relations derived by Holladay, Leung & Coppens (1983), as described elsewhere (Streltsov, Belokoneva, Tsirelson & Hansen, 1993).

For the trigonally distorted FeO_6 octahedron in α-Fe_2O_3, the non-degenerate a_t band is constructed from a d_{z^2} orbital transformed according to an *a* representation (Ballhausen, 1962). For all the other *d* orbitals, e_g and t_{2g} belong to the *e* representation and compose the e_g and e_t bands. The 3*d*-orbital occupancies in α-Fe_2O_3 indicate preferential population of the d_{z^2} and t_{2g} orbitals. The e_g orbital is depopulated significantly in comparison with a spherically averaged free Fe atom. The remaining non-zero population of e_g is an indication of covalent metal–ligand interactions, which is also consistent with the topography of the $\Delta\rho$ distribution maps.

Electron density

$\Delta\rho$ sections based on separate refinements of Zachariasen (1967) type extinction corrections through Fe and O atoms in the $(01\bar{1}0)$ plane for both α-Fe_2O_3 crystals are shown in Figs. 1(*a*) and (*b*). Those through Fe atoms in the $(11\bar{2}0)$ plane and in the (0001) plane for crystal 2 are shown in Figs. 2(*a*) and (*b*). Corresponding maps for the $(01\bar{1}0)$ plane with the parameters for different extinction models included in the structure refinement along with the scale factor are deposited.*

* See deposition footnote.

Table 3. *Atomic charges in electrons from the Hirshfeld partitioning of $\Delta\rho$ and 3d-orbital populations of* Fe *from multipole refinements [crystal (2)] for* α-Fe_2O_3

	Crystal (1)	Crystal (2)	
Fe	0.88 (8)	0.79 (7)	
O	−0.59 (4)	−0.53 (3)	
e_g		1.4 (6) [25.0%]	2.4 [40%]*
t_{2g}		2.2 (6) [36.7%]	2.4 [40%]
d_{z^2}		2.3 (7) [38.3%]	1.2 [20%]
Total		6.0 (3)	6.0

* Spherical atom

The 0.2 e Å^{-3} contour interval is not less than one and a half times the $\sigma(\Delta\rho)$ values presented in Table 1. The $\Delta\rho$ sections shown in Fig. 1 closely resemble the corresponding maps with the preferred extinction correction for α-Al_2O_3 obtained by Maslen,

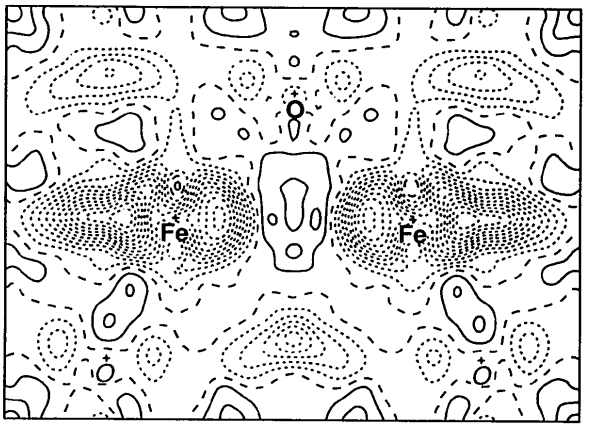

(*a*)

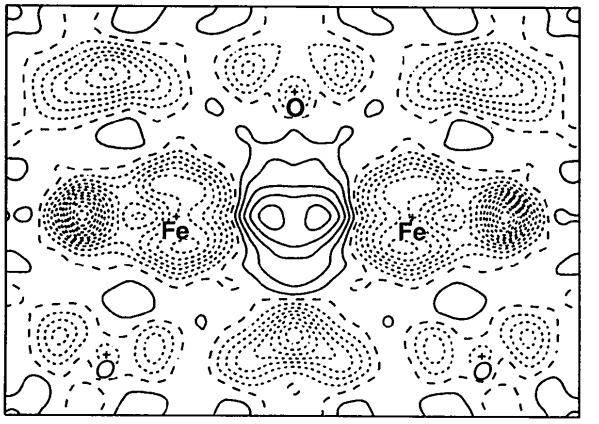

(*b*)

Fig. 1. $\Delta\rho$ for α-Fe_2O_3 in the $(01\bar{1}0)$ plane through two Fe and three O atoms. The two O atoms deviating from the plane by 0.11 Å are shown in italics. (*a*) Crystal (1); (*b*) crystal (2). Map borders: 7.0 × 5.1 Å; contour interval: 0.2 e Å^{-3}; positive and negative contours: solid and short dashes, respectively.

Streltsov, Streltsova, Ishizawa & Satow (1993). The local $\Delta\rho$ symmetry in the vicinity of the Fe atoms in Fig. 2(*b*) approximates sixfold, which is higher than the threefold symmetry expected from the Fe—O bond geometry.

A structure model based on the spherical atoms would predict a deformation density that is locally isotropic around the nuclei. Long range anisotropic $\Delta\rho$ components are not predicted by such a model. Refinement of extinction as part of structure refinement biases the experimental density towards that model. The $\Delta\rho$ symmetries could be lowered by refining extinction corrections with the structure refinement as in previous studies.

The electron density in the vicinity of the metal nuclei is depleted, accumulating near the midpoint of the metal–metal vector along the threefold axis and across the edge of the O-octahedron [Fig. 2(*a*)]. As shown in Fig. 2(*b*), this accumulation extends in a diffuse cloud in a plane normal to *c*, with approximate sixfold symmetry, in contrast with the lower symmetry of the projected O atom positions.

Deformation density features between the Fe atoms strongly support the existence of metal–metal bond interactions, according to the theoretical band-structure considerations proposed by Goodenough (1971). Such cation–cation bonds differ somewhat from the two-centre, two-electron bonds between covalently bonded nearest-neighbour atoms. The a_t and e_t orbitals may form cation sublattice bands by cation–cation interactions along and perpendicular to the *c* axis. The significance of cation–cation interactions affects the $\Delta\rho$ symmetry in the vicinity of the Fe atom, reflecting both the nearest and next-nearest (sixfold) cation coordination in the α-Fe_2O_3 crystal structure.

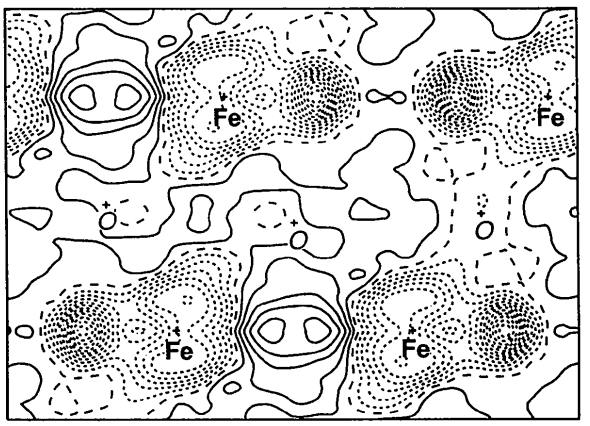

(*a*)

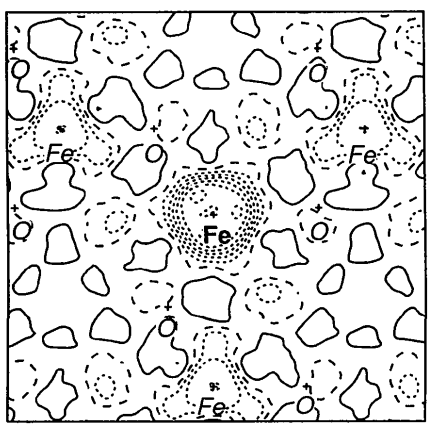

(*b*)

Fig. 2. $\Delta\rho$ for α-Fe_2O_3. Crystal (2). (*a*) In the $(11\bar{2}0)$ plane through Fe atoms with three O atoms deviating from the plane by ± 0.77 and -0.98 Å, shown in italics. Map borders: 7.0×5.1 Å. (*b*) In the (0001) plane through the Fe atom with three Fe atoms deviating from the plane by 0.57 Å and O atoms deviating from the plane by -0.87 Å, shown in italics. Map borders: 6.9×6.9 Å. Contours as for Fig. 1.

This work was supported by the Australian Research Council. Financial support from the Australian National Beamline Facility (ANBF) is also acknowledged. The ANBF is funded by a consortium comprizing the ARC, DITARD, ANSTO, CSIRO, ANU and UNSW. We are indebted to Professor D. C. Creagh for assistance in calculating the absorption and dispersion corrections and to Dr V. A. Murashov for providing the samples.

References

ALCOCK, N. W. (1974). *Acta Cryst.* A**30**, 332–335.
ANTIPIN, M. YU., TSIRELSON, V. G., FLYUGGE, M. P., GERR, R. G., STRUCHKOV, YU. T. & OZEROV, R. P. (1985). *Sov. Phys. Dokl.* **30**(4), 257–258.
BALLHAUSEN, C. (1962). *Introduction to Ligand Field Theory*. New York: McGraw-Hill.
BECKER, P. J. & COPPENS, P. (1974*a*). *Acta Cryst.* A**30**, 129–147.
BECKER, P. J. & COPPENS, P. (1974*b*). *Acta Cryst.* A**30**, 148–153.
CLEMENTI, E. (1965). *IBM J. Res. Dev. Suppl.* **9**, 2.
CREAGH, D. C. (1992). Private communication.
CRUICKSHANK, D. W. J. (1949). *Acta Cryst.* **2**, 65–82.
GOODENOUGH, J. B. (1971). *Prog. Solid State Chem.* **5**, 145–399.
HALL, S. R., FLACK, H. D. & STEWART, J. M. (1992). *Xtal*3.2 *Reference Manual*. Univs. of Western Australia, Australia, and Maryland, USA.
HIRSHFIELD, F. L. (1977). *Isr. J. Chem.* **16**, 198–201.
HOLLADAY, A., LEUNG, P. & COPPENS, P. (1983). *Acta Cryst.* A**39**, 377–387.
LARSON, A. C. (1990). *Crystallographic Computing*, edited by F. R. AHMED. Copenhagen: Munksgaard.
MASLEN, E. N. & SPADACCINI, N. (1993). *Acta Cryst.* A**49**, 661–667.
MASLEN, E. N., STRELTSOV, V. A., STRELTSOVA, N. R., ISHIZAWA, N. & SATOW, Y. (1993). *Acta Cryst.* B**49**, 973–980.
PREWITT, C. T., SHANNON, R. D., ROGERS, D. B. & SLEIGHT, A. W. (1969). *Inorg. Chem.* **8**(9), 1985–1993.
REES, B. (1977). *Isr. J. Chem.* **16**, 180–186.

SATOW, Y. & IITAKA, Y. (1989). *Rev. Sci Instrum.* **60**, 2390–2393.
SPACKMAN, M. A. & STEWART, R. F. (1984). *Methods and Applications in Crystallographic Computing*, edited by S. R. HALL & T. ASHIDA, pp. 302–320. Oxford: Clarendon Press.
STEWART, R. F. & SPACKMAN, M. A. (1983). *VALRAY User's Manual.* Chemistry Department, Carnegie-Mellon Univ., Pittsburgh, PA 15213, USA.
STRELTSOV, V. A., BELOKONEVA, E. L., TSIRELSON, V. G. & HANSEN, N. (1993). *Acta Cryst.* B**49**, 147–153.
STRELTSOV, V. A. & MASLEN, E. N. (1992). *Acta Cryst.* A**48**, 651–653.
TSIRELSON, V. G., ANTIPIN, M. YU., STRELTSOV, V. A., OZEROV, R. P. & STRUCHKOV, YU. T. (1988). *Sov. Phys. Dokl.* **33**(2), 89–91.
VINCENT, M. G., YVON, K. & ASHKENAZI, J. (1980). *Acta Cryst.* A**36**, 808–813.
VINCENT, M. G., YVON, K., GRÜTTNER, A. & ASHKENAZI, J. (1980). *Acta Cryst.* A**36**, 803–808.
ZACHARIASEN, W. H. (1967). *Acta Cryst.* A**23**, 558–564.

Acta Cryst. (1994). B**50**, 441–447

Structure Determination with Laue Diffraction Data – Including Refinement when Anomalous Scatterers are Present

I. M. DODD, QUAN HAO, MARJORIE M. HARDING AND S. M. PRINCE

Chemistry Department, Liverpool University, PO Box 147, *Liverpool L*69 3*BX, England*

(*Received* 20 *September* 1993; *accepted* 22 *December* 1993)

Abstract

The structure of a small single crystal of the organometallic compound $[AuOs_3H(CO)_8\{Ph_2PCH_2P(Ph)C_6H_4\}(PPh_3)]PF_6.0.5C_6H_5Cl$, whose chemical constitution was only partially known, has been determined and refined. Synchrotron radiation with wavelengths in the range 0.24–0.65 Å was used for recording the Laue diffraction patterns from which the reflection intensities were measured. Data processing and initial structure determination followed established procedures. Over this wavelength range, the scattering factors of Au and Os change significantly on account of the anomalous scattering contributions, f' and f''; the program *SHELXL*92 [Sheldrick (1992). *Program for the Refinement of Crystal Structures.* Univ. of Göttingen, Germany] can allow for this variation and with it the structure refinement was completed, giving $R1 = 0.078$, $wR2 = 0.192$ for 10 625 (unmerged) reflection intensities in the space group $C2/c$. Metallation of one phenyl group of the dppm ligand has occurred and the chemical aspects are further discussed by Harding, Kariuki, Mathews, Smith & Braunstein [(1993), *J. Chem. Soc. Dalton Trans.* pp. 33–36]. Synchrotron radiation Laue diffraction data for another organometallic compound, $Ru(C_{12}H_{10}O_4)(C_8H_{11}P)_2(CO)_2$, have also been recorded and used for structure refinement. This crystal of already known structure is non-centrosymmetric, space group $P2_12_12_1$, and provided a further test of the use of wavelength-dependent structure factors in *SHELXL*92. Refinement converged to $R1 = 0.075$, $wR2 = 0.201$ for 7241 reflection intensities and the enantiomorph was unambiguously determined.

Introduction

It is our aim to show that the Laue method for recording diffraction data, with synchrotron radiation, can be used for the complete structure determination of compounds of moderate complexity. The Laue method was, of course, used to establish the structures of many very simple compounds such as sodium chloride (Bragg, 1913; Glusker, 1981). Interest in the application of the Laue method has been revived with the advent of synchrotron radiation, with its continuous range of wavelengths and very high intensity. Helliwell, Habash *et al.* (1989) developed software for deriving reliable reflection intensities from Laue diffraction patterns and such intensity measurements are now being used for protein and virus crystals and for the study of structural changes on a time scale of seconds or less (Helliwell, 1992; Moffat, Chen, Kingman, McRee & Getzoff, 1992). They have also been shown to be sufficient for the structure determination of an organic compound, $C_{25}H_{20}N_2O_2$ (Helliwell, Gomez de Anderez, Habash, Helliwell & Vernon, 1989); structure refinement to $R = 0.053$ for 1914 reflection intensities indicates the quality of data possible. Laue intensity measurements have also been used for the determination of the otherwise unknown structures of three metal